Analytical Potential Energy Surface and Kinetics of the NH3 + H -> NH2 + H-2 Hydrogen Abstraction and the Ammonia Inversion Reactions

ARTICLE *in* THE JOURNAL OF PHYSICAL CHEMISTRY A · MARCH 2010

Impact Factor: 2.69 · DOI: 10.1021/jp1001513 · Source: PubMed

2 AUTHORS:

Joaquin Espinosa-Garcia
Universidad de Extremadura
141 PUBLICATIONS **2,193** CITATIONS
SEE PROFILE

Jose C Corchado
Universidad de Extremadura
118 PUBLICATIONS **3,306** CITATIONS
SEE PROFILE

Analytical Potential Energy Surface and Kinetics of the $NH_3 + H \rightarrow NH_2 + H_2$ Hydrogen Abstraction and the Ammonia Inversion Reactions

J. Espinosa-Garcia* and J. C. Corchado†

Departamento de Química Física, Universidad de Extremadura, Spain

Received: January 07, 2010; Revised Manuscript Received: February 18, 2010

Based on accurate electronic structure calculations, a new analytical potential energy surface (PES) was fitted to simultaneously describe the hydrogen abstraction reaction from ammonia by a hydrogen atom, and the ammonia inversion. Using a wide spectrum of properties of the reactive system (equilibrium geometries, vibrational frequencies, and relative energies of the stationary points, topology of the reaction paths, and points on the reaction swaths) as reference, the resulting analytical PES reproduces reasonably well the input ab initio information obtained at the CCSD(T)/cc-pVTZ level, which represents a severe test for the new surface. As a first application, on this analytical PES we perform an extensive kinetics study using variational transition-state theory with semiclassical transmission coefficients over a wide temperature range, 200−2000 K. For the hydrogen abstraction reaction, the forward rate constants reproduce the experimental measurements, while the reverse ones are slightly underestimated. Another severe test of the new surface is the analysis of the kinetic isotope effects (KIEs). The KIEs between unsubstituted and all deuterated reactions agree with experiment in the common temperature range. For the ammonia inversion reaction, the splitting of the degenerate vibrational levels of the double well due to the tunneling contribution, which is very important in this reaction representing 93% of the reactivity at 200 K, was calculated for the NH_3 and ND_3 species. The values found were 3.6 and 0.37 cm^{-1}, respectively, which although higher than experimental values, reproduce the experimental behavior on isotopic substitution.

I. Introduction

A major challenge in the field of reaction dynamics is to develop quantitatively accurate potential energy surfaces (PES). In the case of polyatomic systems, this is no trivial task, and it is time-consuming. In this context, ammonia presents a rare opportunity to study both intermolecular and intramolecular dynamics.

For the intermolecular case, the gas-phase $NH_3 + H \rightarrow NH_2 + H_2$ reaction is a prototype of the polyatomic hydrogen abstraction reaction. It has been widely studied, using various experimental techniques[1−6] and theoretical methods.[7−17] Experimentally, this reaction seems either to be extremely slow or to give no yield at all at low temperatures,[18,19] but at high temperatures it plays an important role in the chemistry of ammonia pyrolysis and combustion. Theoretically, the reaction has been less studied, although the number of publications has grown in the last five years. The minimum energy path has been calculated by several groups[9,10] using information on electronic structure energy and energy derivatives calculated ab initio, and two potential energy surfaces have been reported, one by our group in 1997,[11] which was the first analytical surface constructed for this reactive system, and another by Moyano and Collins in 2005.[12] In the past few years, on the basis of our PES-1997 (with or without modifications), several groups have performed quantum dynamics calculations with different dimensionality.[13−17] Yang and Corchado[15] observed that a major drawback of the PES-1997 was that it does not describe the inversion of NH_3 correctly. Indeed, PES-1997 predicts wrongly that planar ammonia is more stable (by about 9 kcal mol^{-1}) than the pyramidal structure.

The inversion of ammonia between pyramidal (C_{3v}) and planar (D_{3h}) NH_3 is an example of intramolecular dynamics.[20] This inversion has been widely studied beginning with the pioneer work of Dennisson and Uhlenbeck in 1932,[21] and the first theoretical studies were reviewed by Rauk et al.[22] in 1970. Interest in this intramolecular reaction has continued with the years; different groups have performed theoretical calculations,[23−30] and several potential energy surfaces have been developed.[31−37]

In the present work, to correct the main deficiency of the earlier PES-1997, we report the construction of a new analytical potential energy surface, named PES-2009, which is a fit to very high ab initio calculations. This new surface has the advantage that it simultaneously describes the two important instances of intermolecular and intramolecular dynamics of ammonia, i.e., the hydrogen abstraction reaction with hydrogen, and the pyramidal inversion. The article is structured as follows. In section II, high-level electronic structure calculations are outlined, with special care taken with respect to the information on barrier heights and the topology of the reaction paths (abstraction and inversion). In section III, a detailed description of the PES and the fitting procedure is presented. A severe test of consistency of the new PES is performed in section IV, comparing it with ab initio calculations. The computational details are shown in section V. The kinetics results for both the hydrogen abstraction and the ammonia inversion reactions are presented in section VI, while the dynamics results will be presented in a near future. Finally, section VII presents the conclusions.

II. Electronic Structure Calculations

In this work we develop the PES-2009 that simultaneously describes the hydrogen abstraction and inversion of ammonia.

* Corresponding author. E-mail: joaquin@unex.es.
† E-mail: corchado@unex.es.

10.1021/jp1001513
Published on Web 03/05/2010

TABLE 1: Ab Initio Properties of the Saddle Point for the Abstraction Reaction

parameter	this work[a]	CCSD(T)[b]	MP2[c]
	Geometry		
R(N−H)	1.025	1.022	1.023
R(N−H′)	1.308	1.307	1.305
R(H−H′)	0.890	0.890	0.869
∠N−H′−H	158.4	158.7	158.5
	Energy		
$\Delta E^{\ddagger}$	14.46 (14.73)[d]	15.40	15.44
$\Delta H^{\ddagger}$(0 K)	12.59 (12.86)		
	Vibrational Frequencies		
	3478	3485	3425
	3384	3390	3314
	1888	1908	1973
	1565	1575	1530
	1280	1277	1249
	1063	1125	1089
	677	704	694
	506	672	683
	1662i	1624i	1920i

[a] Calculations at the CCSD(T)/cc-pVTZ level. Distances in Å, angles in degrees, relative energies in kcal mol^{-1}, and frequencies in cm^{-1}. [b] Reference 44. [c] Reference 10. [d] In parentheses, values using the IB method (see text).

For the fitting process, the input information is exclusively based on very high-level ab initio calculations describing the topology of both reactions from reactants to products, with special care taken in the description of the reaction paths and reaction swaths.

In the present work we took the singles and doubles coupled-cluster approach including a quasi-perturbative estimate of the connected triple excitations, correlating only valence electrons, CCSD(T), using the correlation consistent polarized triple-ζ basis set, cc-pVTZ,[38] abbreviated CCSD(T)/cc-pVTZ level. For both paths, abstraction and inversion, we optimized and characterized all the stationary point geometries (reactants, products, and saddle points), and constructed the minimum energy paths (MEP) at this ab initio level over a broad range of the respective reaction coordinates. Moreover, we calculated the bending motion of the abstraction saddle point, because Schatz et al.[39,40] showed that surfaces having the same saddle point but different dependences of the energy on the bending angle presented different dynamics results, for instance, different rotational excitations in the products. Calculations were performed using the GAUSSRATE code,[41] which serves as an interface between the GAUSSIAN03 systems of programs[42] and POLYRATE.[43]

Doubtless, one of the most difficult energy properties of a PES to estimate accurately is the barrier height. The ab initio calculations at the CCSD(T)/cc-pVTZ level are listed in Tables 1 and 2 for the abstraction and inversion reactions, respectively, together with other theoretical values from the literature for comparison. It is well-known that the classical barrier height is strongly dependent on the basis set. Therefore, we use the "infinite-basis" (IB) method of Truhlar et al.[45,46] for extrapolation to a complete one-electron basis set, which is based on correlation consistent polarized double- and triple-ζ basis sets. The single-point calculations with the IB method are also listed in Tables 1 and 2.

For the hydrogen abstraction reaction, $NH_3 + H \rightarrow NH_2 + H_2$, the bond lengths being formed (H−H′) and broken (N−H′) at the saddle point (where H′ is the transferring H atom) are in the narrow ranges 1.022−1.025 and 1.305−1.308 Å, respectively, with the barrier height in the narrow range 14.73−15.44 kcal mol^{-1}.

TABLE 2: Ab Initio Properties of the Stationary Points for the Inversion Reaction

parameter	this work[a]	LCH[b]	HRG[c]	RW[d]
	Geometry Pyramidal NH_3			
R(N−H)	1.014	0.994	1.011	1.013
dihedral angle	111.7		106.0	
	Vibrational Frequencies			
	3600		3656	
	3600		3656	
	3473		3512	
	1687		1686	
	1687		1686	
	1108		1086	
	Geometry planar NH_3			
R(N−H)	0.995	1.011	0.994	0.998
dihedral angle	180.0	180.0	180.0	180.0
	Energy			
$\Delta E^{\ddagger}$	6.40 (5.20)[e]	5.05	5.94	5.51
$\Delta H^{\ddagger}$(0 K)	5.54 (4.34)		5.04	
	Vibrational Frequencies			
	3866		3899	
	3866		3899	
	3655		3678	
	1586		1589	
	1586		1589	
	900i		878i	

[a] Calculations at the CCSD(T)/cc-pVTZ level. Distances in Å, angles in degrees, relative energies in kcal mol^{-1}, and frequencies in cm^{-1}. [b] Reference 37. [c] Reference 30. [d] Reference 27. [e] In parentheses, values using the IB method (see text).

In the inversion reaction, the planar NH_3 presents bond lengths in the range 0.994−1.011 Å, with the barrier height in the range 5.20−5.94 kcal mol^{-1}, and the imaginary frequency being estimated at between 878 and 900 cm^{-1}. In this case, the effect of the basis set extrapolation is noticeable, decreasing the barrier from 6.40 to 5.20 kcal mol^{-1}.

III. Analytical PES Function and Fitting Procedure

The analytical PES function we employ is based on our old PES-1997 surface.[11] This is basically a valence bond-molecular mechanics (VB-MM) surface, given by the sum of three terms: a valence bond stretching potential, $V_{stretch}$, and two molecular mechanics terms, a harmonic bending term, V_{harm}, and an anharmonic out-of-plane potential, V_{op},

$$V = V_{stretch} + V_{harm} + V_{op} \quad (1)$$

and it was designed to describe exclusively the hydrogen abstraction reaction. The functional form was developed in that paper and will be not repeated here. The V_{op} term was added to obtain a correct description of the umbrella mode of ammonia. Recently, however, Yang and Corchado[15] noted that this term leads to unphysical behavior along the ammonia inversion path (which originally was not taken into account).

To avoid this drawback, and to describe simultaneously both the hydrogen abstraction and the inversion reactions, in the present work we develop the new PES function as the sum of only the stretching and harmonic bending terms,

$$V = V_{stretch} + V_{harm} \quad (2)$$

and a series of switching functions allowing the smooth change from pyramidal NH_3 to NH_2 product in the hydrogen abstraction reaction, and from pyramidal to planar NH_3 in the inversion path. In total, 14 and 16 parameters for the stretching and

harmonic bending terms, respectively, are required to describe the surface. The new PES, PES-2009, therefore depends on 30 parameters that give it great flexibility while keeping the VB-MM functional form physically intuitive. This PES is symmetric with respect to the permutation of the ammonia hydrogen atoms, a feature especially interesting for dynamics calculations.

Using as input information exclusively high-level ab initio calculations at the CCSD(T)/cc-pVTZ level, describing all the stationary points and the respective reaction paths and reaction swaths for the two paths described in this paper, we fitted the 30 parameters describing the new PES-2009. We used a multibeginning least-squares procedure developed recently in our group.[47] In brief, we use the very popular least-squares method to fit an analytical function depending on m parameters, $p = (p_1, ..., p_m)$. One must note, however, that any fitting procedure has certain limitations. First, it is very hard to find a global minimum for the fit; second, the final result is dependent on the initial parameters; third, one usually obtains a number of distinct sets of parameters, all equally probable and good; and fourth, to make matters worse, while the differences between these parameters sets may be small, the kinetic and dynamic information obtained from them can vary noticeably. To solve at least partially some of the above problems, we developed a hybrid algorithm to perform the fit. This algorithm has two steps. The first of them is to use Powell's method for local optimization, and the second is to apply a multibeginning method to search for a global optimum.

In that work[47] we observed that the approach is unsuccessful if all the theoretical information is introduced as input and all the adjustable parameters are allowed to optimize simultaneously, because the problem is ill-conditioned, and also because the large number of free parameters leads to an enormous space of possibilities for the optimization algorithm to explore. So, we developed a step-by-step fitting process (divide-and-conquer strategy) based on the physical meaning of the adjustable parameters. In brief, the fitting procedure used in this work has the following steps.

1. We establish the parameters of the PES related to the geometric, energy, and vibrational properties of the reactants and products, so that the geometries, classical reaction energy, and vibrational frequencies reproduce the reference ab initio CCSD(T)/cc-pVTZ level values. We also fit the values of the parameters of the switching functions that describe changes along the reaction paths.

2. Now we fit the remaining parameters to reproduce the characteristics of the ab initio calculations for the saddle points (in particular, the geometry, barrier height, and vibrational frequencies), the reaction paths and reaction valleys (taking special care to ensure that no artificial deep wells were introduced into the reactant or product valleys), and the reaction swaths.

3. With these steps we obtain a first set of parameters that are used as the starting point for the next fit. We test whether a new fit of the parameters would improve the results, and the process is continued until no further changes are detected. The resulting parameter values were taken as the best values of this fitting algorithm.

IV. Test of Consistency of the New PES: Comparison with ab Initio Calculations

We begin analyzing the newly constructed PES-2009, testing its consistency. In particular, in the present section we analyze to what extent the reference information used for the fit, computed at the CCSD(T)/cc-pVTZ level, can be reproduced. Table 3 lists the values of geometries, vibrational frequencies, and energies at the stationary points for the two paths, abstraction and inversion. In general, the agreement between PES and ab initio values is reasonable, with the most significant differences being the N−H′−H bend angle at the saddle point for the abstraction reaction. While the ab initio calculations yield a nonlinear angle, 158.4°, the PES yields a collinear approach, which is the expected behavior of the LEP-type (London−Eyring−Polanyi) function used to describe the stretching term in the potential (eq 2). A priori, one would think that it might be possible to use LEP-type surfaces to describe the kinetics and dynamics of systems with noncollinear reaction paths. Two previous papers from our group[48,49] analyzed this possibility, using the atom−diatom Cl + HCl and the polyatomic $O(^3P) + NH_3$ reactions as models, which present a "bent" structure of the saddle points with ab initio calculations, 161.4° and 159.5°, respectively. They indeed showed that the collinear LEP-type surfaces and the ab initio "bent" surfaces present similar kinetics and dynamics behavior. This capability of the LEP-type surfaces to reproduce the kinetics and dynamics of polyatomic systems with noncollinear reaction paths is encouraging and represents a great saving in computational time.

With respect to the reaction enthalpy at 0 K, $\Delta H_R(0K)$, the PES-2009 value reproduces the ab initio reference, with a difference of 0.6 kcal mol^{-1}. Moreover, for the abstraction reaction, the PES enthalpy, 1.74 kcal mol^{-1}, is within the experimental uncertainty, 2.1 ± 0.6 kcal mol^{-1} (see section VI.A for a more detailed discussion of this value).

Figure 1 plots energy changes along the reaction path for the abstraction (panel a) and inversion (panel b) reactions. With respect to the reference ab initio level, CCSD(T)/cc-pVTZ, the energy changes along the reaction paths for the abstraction and inversion reactions are reasonably well described, with the largest differences being about 1 kcal mol^{-1} in the exit channel for the abstraction reaction. In both paths, the improvements with respect to the old PES-1997 surface are especially notable for the inversion reaction, where the PES-1997 presented a nonphysical behavior, with a minimum at the saddle point of about 9 kcal mol^{-1} with respect to the reactant.

Figure 2 shows the energy as a function of the N−H′−H angle for the abstraction reaction, keeping the remaining parameters at the saddle point geometry at the reference level. The fitted PES reproduces the ab initio information in the wide angle range 90−180°. Note that there is a slight deviation in the location of the minimum of this curve, with the fitted PES having its minimum at 180°.

Finally, contour plots in the proximity of the saddle points for the reference ab initio and the fitted PES are shown in Figures 3 and 4 for the hydrogen abstraction and inversion reactions, respectively. In both cases, the fitted surface reproduces the reaction path, reaction valley, and reaction swath from the ab initio information. This behavior is especially interesting for the following kinetics and dynamics studies (see below).

V. Computational Details

With the new PES-2009 surface, developed to describe both abstraction and inversion reactions, the reaction paths were calculated starting from the respective saddle point geometry and moving downhill to both reactants and products in mass-weighted Cartesian coordinates using Page and McIver's method,[50] obtaining the minimum energy path, MEP.[51] Along both MEPs, we calculated vibrational frequencies after having projected out the motion along the reaction path using redundant

TABLE 3: Properties of the Stationary Points for Both Reactions[a]

	geometry		frequency		ΔV		ΔH(0K)	
parameter	PES	ab initio	PES	ab initio	PES	ab initio	PES	ab initio
			NH_3 (C_{3v}), Pyramidal					
R(N−H)	1.012	1.014	3606	3600				
∠HNH	109.0	105.6	3606	3600				
			3478	3473				
			1630	1687				
			1630	1687				
			1112	1108				
			NH_3 (D_{3h}), Planar					
R(N−H)	1.012	0.995	3622	3866	4.87	5.20	3.77	4.34
∠HNH	120.0	120.0	3622	3866				
			3422	3655				
			1812	1586				
			1812	1586				
			903i	900i				
			NH_2					
R(N−H)	1.012	1.026	3443	3458	5.00	4.42	1.74	1.04
∠HNH	103.4	102.2	3395	3366				
			1462	1558				
			Abstraction Saddle Point					
R(N−H)	1.013	1.025	3444	3478	14.48	14.73	13.08	12.86
R(N−H′)	1.279	1.308	3373	3384				
R(H−H′)	0.868	0.890	1861	1888				
dihedral angle	180.0	158.4	1623	1566				
			1497	1280				
			1080	1063				
			622	677				
			581	506				
			1602 *i*	1662 *i*				

[a] Calculations at the CCSD(T)/cc-pVTZ level. Distances in Å, angles in degrees, relative energies in kcal mol^{-1}, and frequencies in cm^{-1}.

internal coordinates.[52,53] With this information, we calculated the respective ground-state vibrationally adiabatic potential curve,

$$V_a^G(s) = V_{MEP}(s) + \varepsilon_{int}^G(s) \quad (3)$$

where $V_{MEP}(s)$ is the classical energy along the MEP with its energy zero at the reactants, and $\varepsilon_{int}^G(s)$ is the zero-point energy at s. Rate constants were estimated using canonical variational transition-state theory (CVT).[54,55] Quantum effects in motions orthogonal to the reaction path were included by using quantum-mechanical vibrational partition functions in the harmonic approximation, and those in the motion along the reaction path by using the microcanonical optimized multidimensional tunneling (μOMT) approach[43] in which, at each total energy, the larger of the small-curvature (SCT) and large-curvature (LCT) tunneling probabilities is taken as the best estimate. We used the centrifugal-dominant SCT[56] and version-4 LCT[57] methods. In all the cases, the SCT tunneling probabilities were larger, indicating that SCT tunneling is an adequate approximation for computing tunneling in this reaction. All kinetic calculations were performed using the general polyatomic rate constant code POLYRATE,[43] in which the rotational partition functions were calculated classically.

VI. Results and Discussion

As a first application of the new PES, in this paper we present the kinetics results using the variational transition-state theory with inclusion of multidimensional tunnelling corrections.

(A) Hydrogen Abstraction Reaction, $NH_3 + H \rightarrow NH_2 + H_2$. Table 4 lists the variational CVT/μOMT forward rate constants in the temperature range 200−2000 K obtained with

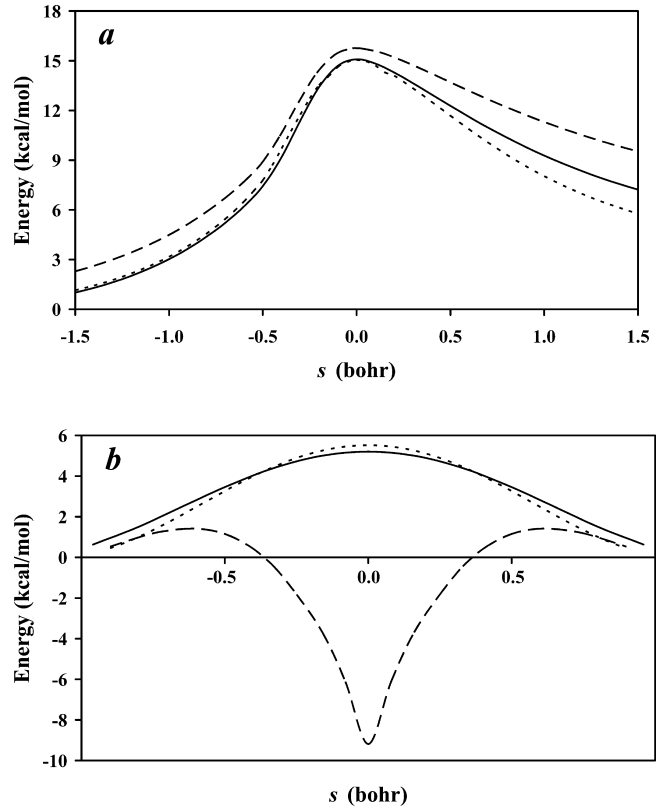

Figure 1. Classical potential energy as a function of the reaction coordinate, s: (a) hydrogen abstraction reaction; (b) ammonia inversion. The curves are PES-2009 (solid line), PES-1997 (dashed line), and CCSD(T)/cc-pVTZ (dotted line).

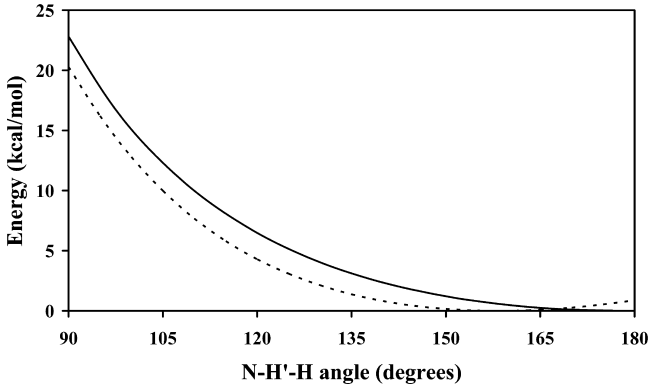

Figure 2. Changes in the energy of the saddle point (optimized at the CCSD(T)/cc-pVTZ level) as the N−H′−H_B angle is bent from linear to 90°. The zero of energy is set at the energy of the saddle point geometry optimized at the CCSD(T)/cc-pVTZ level. Dotted line: CCSD(T)/cc-pVTZ energies. Solid line: PES-2009 energies.

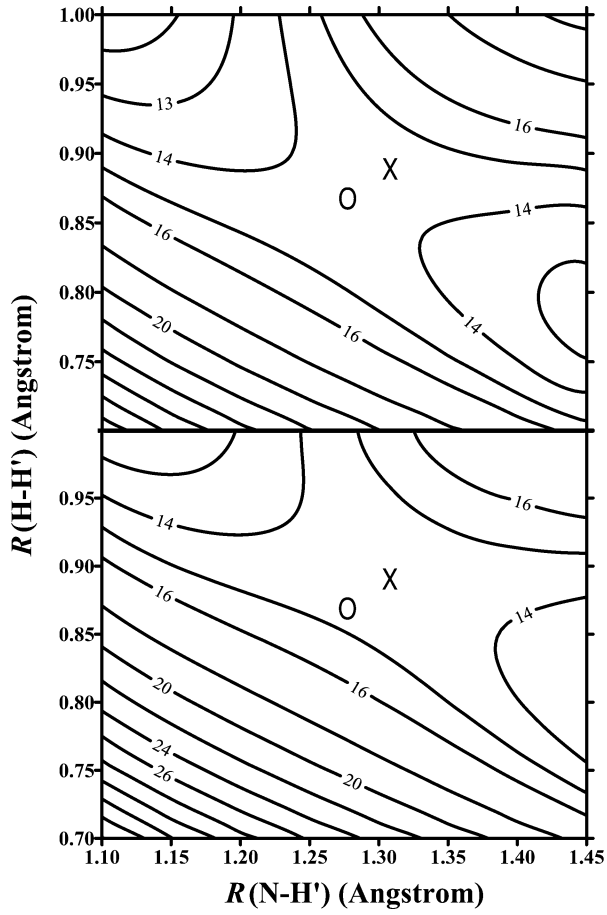

Figure 3. Hydrogen abstraction reaction. Contour plots of the analytical PES-2009 (upper panel) and CCSD(T)/cc-pVTZ surface (lower panel) in the proximity of the saddle point. The symbol X indicates the location of the CCSD(T)/cc-pVTZ saddle point, while the symbol O is the saddle point in the analytical PES.

the PES-2009 surface, together with experimental[5] and other theoretical values[11,15,17] for comparison. Figure 5 shows the corresponding Arrhenius plots. The PES-2009 kinetic results reproduce the experimental evidence over the common temperature range, 500−2000 K. Note that the present results improve the PES-1997 rate constants,[11] especially at low temperatures ($T \leq 500$ K), while both surfaces reproduce the experimental behavior at high temperatures. Seven-dimensional (7D)[15] and full-dimensional (FD)[17] time-dependent wave packet

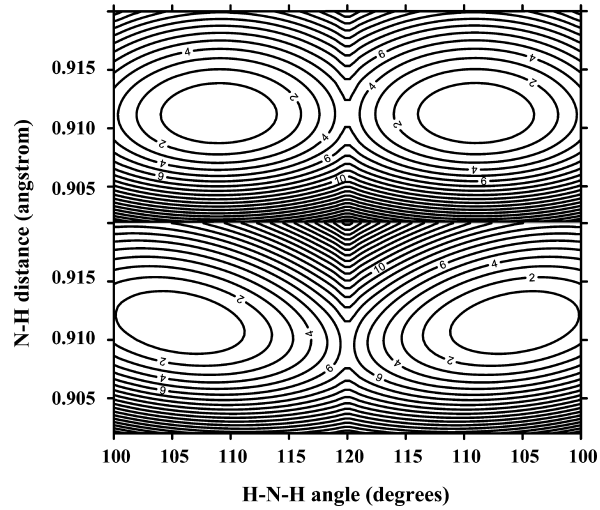

Figure 4. Ammonia inversion reaction. Contour plots of the analytical PES-2009 (upper panel) and CCSD(T)/cc-pVTZ surface (lower panel).

(TDWP) calculations were performed on the old PES-1997, modified to avoid the spurious well in the inversion reaction at the saddle point. The corresponding rate constants are underestimated by factors between 11 (200 K) and 4.6 (2000 K) for the 7D calculation, and between 3.8 (200 K) and 1.5 (2000 K) for the FD one, with respect to the present calculations.

The PES-2009 reverse rate constants, CVT/μOMT, are listed in Table 5 for the temperature range 200−2000 K, together with experimental[6,58,59] and other theoretical results[11,16] for comparison, and the Arrhenius plot is shown in Figure 6. The PES-2009 results underestimate the experimental values[58,59] by up to a factor of 2.7 at 400 K, and this disagreement is somewhat larger if the most recent experimental values[6] are taken as reference.

The equilibrium constants (K_{eq}) are calculated in the transition-state theory approach based only on reactant and product properties, and hence the reaction path properties cancel out. Table 6 lists the K_{eq} values in the temperature range 400−2000 K together with the JANAF values[60] obtained from thermochemical calculations,

$$K_{eq} = \exp\left(-\frac{\Delta H_R^o}{RT} + \frac{\Delta S_R^o}{R}\right) \quad (4)$$

where ΔH_R^o is the enthalpy of reaction and ΔS_R^o is the entropy of reaction, and with the few existing experimental values[4,59] obtained from kinetics measurements.

The K_{eq} value obtained from thermochemical data depends on the standard enthalpy of reaction, ΔH_R^o, which can be obtained from the corresponding standard enthalpies of formation, ΔH_f^o, of reactants and products. While the ΔH_f^o values of NH_3, H, and H_2 are well established,[60] the proposed experimental values of the enthalpy of formation of the NH_2 free radical present discrepancies. In particular, they vary between 44.0 ± 2.3 (ref 62) and 48.1 ± 3.5 (ref 63) kcal mol^{-1}, although the latest compilations diminish this range. Thus, for instance, the JANAF tables[60] recommend 45.5 ± 1.5 kcal mol^{-1}, which agrees with a recent experimental determination.[6] However, recent theoretical[64] and experimental[65] works reduce this value by one unit, 44.6 ± 0.1 and 44.5 ± 0.1 kcal mol^{-1}, respectively, which agree with our theoretical value,[61] 43.8 ± 0.6 kcal mol^{-1} within the uncertainties. Therefore, although the enthalpy of formation of the NH_2 product seems still an open question, this

TABLE 4: Rate Constants and μOMT Transmission Coefficients for the $NH_3 + H \rightarrow NH_2 + H_2$ Abstraction Reaction[a]

T (K)	PES-2009	μOMT	exp[b]	PES-1997[c]	YC(7D)[d]	Y(FD)[e]
200	1.10×10^{-23}	133.1		6.17×10^{-24}	1.86×10^{-24}	5.54×10^{-24}
300	5.78×10^{-20}	7.5		2.50×10^{-20}	7.79×10^{-21}	1.44×10^{-20}
400	7.42×10^{-18}	3.0		3.48×10^{-18}	1.34×10^{-18}	1.08×10^{-18}
500	1.65×10^{-16}	2.0	1.25×10^{-16}	8.66×10^{-17}	3.90×10^{-17}	1.97×10^{-17}
600	1.43×10^{-15}	1.6	1.02×10^{-15}	8.29×10^{-16}	3.99×10^{-16}	1.56×10^{-16}
700	7.09×10^{-15}	1.4	4.85×10^{-15}	4.46×10^{-15}	2.17×10^{-15}	7.33×10^{-16}
1000	1.50×10^{-13}	1.2	9.70×10^{-13}	1.12×10^{-13}	4.74×10^{-14}	1.37×10^{-14}
1200	5.35×10^{-13}	1.1	3.45×10^{-13}	4.34×10^{-13}	1.59×10^{-13}	4.55×10^{-14}
1500	2.08×10^{-12}	1.1	1.35×10^{-12}	1.84×10^{-12}	5.32×10^{-13}	1.59×10^{-13}
2000	9.09×10^{-12}	1.0		8.90×10^{-12}	1.80×10^{-12}	5.90×10^{-12}

[a] CVT/μOMT, in cm^3 $molecule^{-1}$ s^{-1}. [b] From ref 5. $k(T) = 9.0 \times 10^{-19} T^{2.40} \exp(-4991/T)$, $T = 490-1780$ K. [c] Reference 11. CVT/μOMT calculations. [d] Reference 15. Seven-dimensional TDWP calculations using a modified PES-1997 surface. [e] Reference 17. Full-dimensional TDWP calculations using a modified PES-1997 surface.

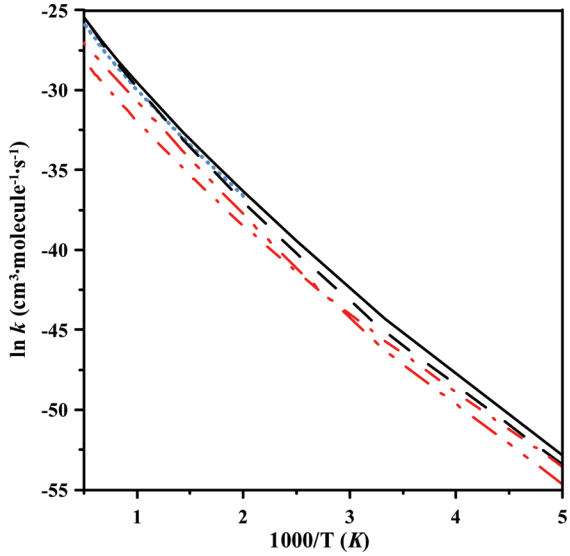

Figure 5. Arrhenius plots of ln k (cm^3 $molecule^{-1}$ s^{-1}) for the forward thermal rate constants against the reciprocal of temperature (K) in the range 250−2000 K: solid black line, PES-2009; dashed black line, PES-1997; dotted blue line, experimental values from ref 5; dashed-dotted-dotted red line, seven-dimensional TDWP results from ref 15; dashed-dotted red line, full-dimensional TDWP results from ref 17.

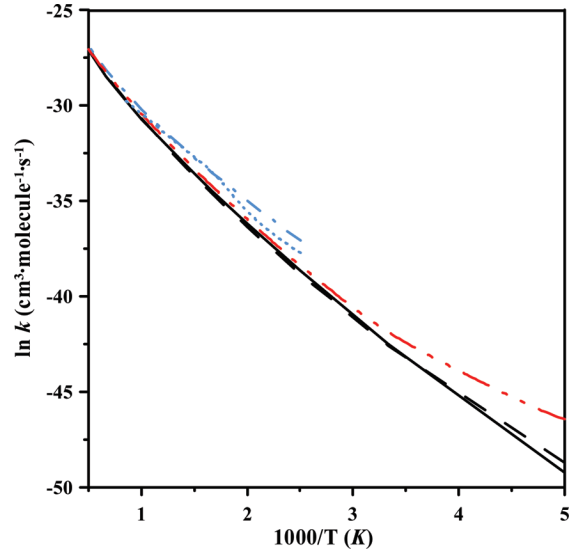

Figure 6. Same as Figure 5, but for the reverse reaction, $H_2 + NH_2 \rightarrow H + NH_3$: solid black line, PES-2009; dashed black line, PES-1997; dotted blue line, experimental values from refs 58 and 59; dashed-dotted blue line, experimental values from ref 6; dashed-dotted-dotted red line, seven-dimensional TDWP results from ref 16.

value doubtless strongly influences the standard enthalpy of reaction, and hence the equilibrium constants (eq 4). For instance, a decrease of 1 kcal mol^{-1} increases K_{eq} by a factor of from ≈5 at 400 K to ≈2 at 1000 K. With these considerations in mind, our results show reasonable agreement with the experimental values, being overestimated by a factor maximum of 3 over the temperature range 400−2000 K.

The phenomenological activation energies at 298 K (from slopes of Arrhenius plots from 293 to 303 K) are 11.08 and 8.75 kcal mol^{-1} for the forward and reverse reactions, respectively. In this case, the reaction path properties are considered, instead of just the reactant and product properties as in the K_{eq} calculation. Using these values and the second law derivation, $\Delta H_R^0(298K) = E_a(f) - E_a(r)$, the standard reaction enthalpy is 2.3 kcal mol^{-1}. Given that the standard enthalpies of formation

TABLE 5: Rate Constants for the $NH_2 + H_2 \rightarrow NH_3 + H$ Abstraction Reaction[a]

T (K)	PES-2009	exp[b]	exp[c]	PES-1997[d]	YC(7D)[e]
200	4.16×10^{-22}			6.80×10^{-22}	6.65×10^{-21}
300	3.39×10^{-19}			3.16×10^{-19}	6.47×10^{-19}
400	1.60×10^{-17}	4.13×10^{-17} [f]	7.89×10^{-17}	1.35×10^{-17}	2.13×10^{-17}
500	1.88×10^{-16}	3.63×10^{-16} [f]	6.33×10^{-16}	1.60×10^{-16}	2.42×10^{-16}
600	1.05×10^{-15}	2.86×10^{-15}	2.77×10^{-15}	9.22×10^{-16}	1.37×10^{-15}
700	3.80×10^{-15}	8.52×10^{-15}	8.47×10^{-15}	3.44×10^{-15}	5.03×10^{-15}
1000	4.58×10^{-14}	6×10^{-14}	7.77×10^{-14}	4.68×10^{-14}	6.11×10^{-14}
1200	1.34×10^{-13}		2.06×10^{-13}	1.36×10^{-13}	1.75×10^{-13}
1500	4.36×10^{-13}		6.07×10^{-13}	4.64×10^{-13}	5.36×10^{-13}
2000	1.69×10^{-12}		2.12×10^{-12}	1.89×10^{-12}	1.79×10^{-12}

[a] CVT/μOMT, in cm^3 $molecule^{-1}$ s^{-1}. [b] From ref 59. $k(T) = 5.98 \times 10^{-12} \exp(-9082 \pm 717/RT)$, $T = 673-1003$ K. [c] From ref 6. [d] Reference 11. CVT/μOMT calculations. Note that the present values do not correspond with the original values. This is because the reaction path degeneracy factor was wrongly set to 2, instead of 4. [e] Reference 16. Seven-dimensional TDWP calculations using a modified PES-1997 surface. [f] From ref.[58]

TABLE 6: Equilibrium Constants for the $NH_3 + H \rightarrow NH_2 + H_2$ Reaction[a]

T (K)	PES-2009	JANAF[b]	exp[c]	exp[d]	PES-1997[e]
400	0.46	0.16 (1.56)			0.25
500	0.88	0.44 (2.73)			0.52
600	1.36	0.85 (3.86)			0.88
700	1.86	1.13 (4.13)	0.13−1.45		1.27
1000	3.27	1.79 (4.43)	0.62−3.31	1.17	2.41
1200	4.00	1.88 (4.00)		1.37	3.16
1500	4.76	1.90 (3.48)		2×10	3.92
2000	5.39	1.72 (2.70)			4.67

[a] CVT/μOMT calculations. [b] Reference 60. Values of enthalpy of reaction obtained using the NH_2 enthalpy of formation $\Delta H_{f,0K} = 46.2 \pm 1.5$ kcal mol^{-1} or $\Delta H_{f,298K} = 45.5 \pm 1.5$ kcal mol^{-1}. In parentheses the values obtained using our NH_2 enthalpy of formation,[61] $\Delta H_{f,0K} = 44.4 \pm 0.6$ kcal mol^{-1} or $\Delta H_{f,298K} = 43.8 \pm 0.6$ kcal mol^{-1}. [c] Reference 19. [d] Reference 4. [e] Reference 11. CVT/μOMT calculations. Note that the present values do not correspond with the original values. This is because for the reverse reaction the reaction path degeneracy factor was wrongly set to 2, instead of 4. Therefore, the values in this table are half those in the original paper.

TABLE 7: Kinetic Isotope Effects for the Forward Reaction[a]

T (K)	PES-2009	exp[b]	G[c]	PES-1997[d]
500	2.87	[2.46]		3.51
600	2.48	2.32	3.79	2.83
700	2.24	2.25		2.45
1000	1.87	2.1	2.18	1.92
1200	1.75	2.04		1.75
1500	1.54	[1.97]	1.73	1.61

[a] $NH_3 + H$ versus $ND_3 + D$ rate constants with CVT/μOMT calculations. [b] $k(NH_3+H) = (5.7 \pm 2.8) \times 10^{-10} \exp[-(8650 \pm 410)/T]$ (cm^3 molecule^{-1} s^{-1}) (ref 3); $k(ND_3+D) = 3.2 \times 10^{-10} \exp(-8810/T)$ (cm^3 molecule^{-1} s^{-1}) (ref 66). The values in brackets are extrapolations. [c] Reference 9. [d] Reference 11. CVT/μOMT calculations.

TABLE 8: Kinetic Isotope Effects for the Reverse Reaction[a]

T (K)	PES-2009	G[b]	PES-1997[c]
500	2.35		2.46
600	2.21	2.91	2.22
700	2.10		2.06
1000	1.87	2.06	1.79
1200	1.77		1.68
1500	1.66	1.68	1.58

[a] $NH_2 + H_2$ versus $ND_2 + D_2$ rate constants with CVT/μOMT calculations. [b] Reference 9. [c] Reference 11. CVT/μOMT calculations.

of NH_3 and H are well established,[60] -10.97 ± 0.1 and 52.10 kcal mol^{-1}, respectively, we obtain a value for the NH_2 product of $\Delta H_{f,298K} = 43.4$ kcal mol^{-1}. This value agrees with our theoretical value,[61] 43.8 ± 0.6 kcal mol^{-1}, and recent theoretical[64] and experimental[65] values, suggesting that the compiled value[60] may be overestimated by about 1 kcal mol^{-1} at least.

The kinetic isotope effects (KIE) provide another severe test of several features of the new surface (barrier height and width, zero-point energy near the dynamic bottleneck, and tunneling effects). Unfortunately, there is a limited number of theoretical[9] and experimental[66] results for comparison. The calculated KIEs at different temperatures for the unsubstituted ($NH_3 + H$) and all-substituted ($ND_3 + D$) reactions are listed in Tables 7 and 8 for the forward and reverse reactions, respectively.

The KIEs for the forward reaction show excellent agreement with the available experimental values,[3,66] decreasing when the temperature increases. The present results improve the old PES-1997 results, especially at low temperatures. For the reverse reaction, to the best of our knowledge no experimental data are available, and only two theoretical calculations have been reported.[9,11] The agreement with the values reported by Garrett et al.[9] is surprising given the great differences between the individual rate constants used in the two works.

TABLE 9: Thermal Rate Constants for the Ammonia Inversion (in s^{-1})

	NH_3		ND_3	
T (K)	CVT	CVT/μOMT	CVT	CVT/μOMT
200	3.22×10^8	6.31×10^9	1.61×10^8	8.31×10^8
300	1.12×10^{10}	3.78×10^{10}	7.00×10^9	1.68×10^{10}
400	7.05×10^{10}	1.39×10^{11}	4.83×10^{10}	9.09×10^{10}
500	2.19×10^{11}	3.34×10^{11}	1.57×10^{11}	2.58×10^{11}

In sum, the agreement between the hydrogen abstraction kinetics results obtained and experiment (forward and reverse rate constants, equilibrium constants, and KIEs) lends confidence to the PES constructed in this work, which noticeably improves the results obtained with the old PES-1997 surface.

(B) Ammonia Inversion Reaction, NH_3 (C_{3v}) ↔ NH_3 (D_{3h}). The inversion of ammonia is the paradigm of intramolecular transformations, where one pyramidal (C_{3v}) structure of ammonia transforms into the other through a planar (D_{3h}) saddle point.

We begin by analyzing the kinetics results. First we computed the thermal rate constants in the temperature range 200−500 K using the CVT/μOMT method on the PES-2009 surface. These rates are listed in Table 9 for ammonia and the deuterated isotope. We would like to stress that these calculations are included only for completeness, since the ammonia inversion is too fast to allow the reactants or products of this reaction to thermalize. In fact, from these results we can see that even at low temperature, the ammonia inversion is very fast, on the order of 10^{10} times per second, and the tunneling contribution computed semiclassically is very important in this reaction. Thus, tunneling accounts for between 93% and 29% of the reactivity in the temperature range 200−500 K.

Next, the ammonia splitting is analyzed. The inversion motion is represented by a symmetric double-well potential. As a consequence of the perturbation originating this double well, a splitting of each degenerate vibrational level into two levels appears, ΔE, due to quantum mechanical tunneling,[20] and the splitting increases rapidly with the vibrational number.[67] For the NH_3 ground state, this splitting has been experimentally measured and is very small, 0.66 (ref 67), 0.79 (ref 68), or 0.8 (ref 69) cm^{-1}. Figure 7 plots this path for ammonia where the first two pairs of split eigenvalues are superimposed.

We computed tunneling splitting for our PES using a semiclassical reaction-path method[24] with the SCT tunneling probabilities. Thus, the splitting ΔE can be computed from the tunnelling rate of inversion, k_{tunn}, which is in turn obtained from the imaginary action integral, $\theta(E)$, using the WKB approximation[30]

$$\Delta E_0 = \frac{k_{tunn}}{2c} \tag{5}$$

$$k_{tunn} = \frac{2c\nu_2}{\pi} \exp[-\theta(E)] \tag{6}$$

c being the speed of light and ν_2 the eigenvalue associated with the inversion mode of ammonia, 1113 cm^{-1}. The imaginary action integral is obtained using the SCT method. The computed

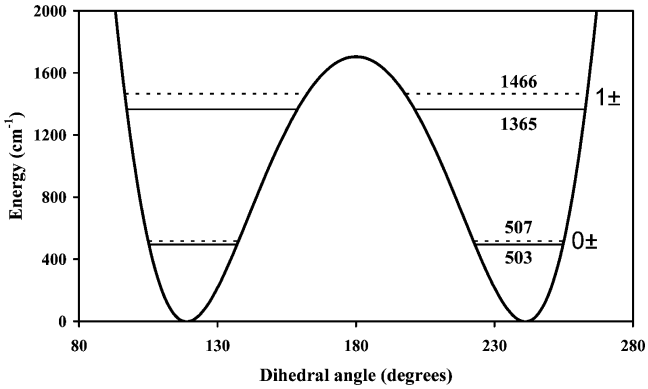

Figure 7. Classical potential for NH_3 obtained from the PES-2009 surface. The first two pairs of eigenvalues are shown.

TABLE 10: Eigenvalues of Ammonia Inversion (in cm^{-1})

ν_2	PES-2009	exp[a]	HG[b]
0^+	0.00	0.00	0.00
0^-	3.64	0.79	1.17
1^+	861.39	932.43	921.25
1^-	962.90	968.12	976.64
2^+	1533.36	1598.47	1572.27
2^-	1942.29	1822.18	1921.06

[a] Reference 35. [b] Reference 29. Ab initio calculations at the MP4(SDQ)/aug-cc-pVTZ level.

splittings are listed in Table 10 together with experimental[35] and other theoretical[29] values for comparison. The PES-2009 results overestimate the experiment and the other theoretical values. Although more sophisticated methods exist for the computation of tunneling splitting,[70−72] the method used here has shown itself to be accurate enough to give a more reasonable value than the one we actually found. Therefore, the reason for the discrepancy mainly lies in the shape of the PES, although other factors such as the tunnelling calculation cannot be discarded. Indeed, we found that the overestimate we obtain in tunneling splitting is due to our barrier to inversion being slightly lower and thinner than that of other studies. Unfortunately, tunneling splitting is so sensitive to the shape of the PES that a few tenths of kcal·mol^{-1} give rise to a factor of 4 in the computed splitting. With respect to the effect of isotopic substitution, for the ND_3 case we obtain a value $\Delta E = 0.37$ cm^{-1}. Although this is greater than the experimentally reported value, 0.05 cm^{-1},[73] it correctly predicts the about 1 order of magnitude reduction upon isotopic substitution.

VII. Conclusions

We have presented the construction of a new analytical potential energy surface describing simultaneously the reactions of hydrogen abstraction in $NH_3 + H$ and of ammonia inversion. The method was based on taking an analytical function developed by our group, and performing a multibeginning least-squares optimization of the parameters. The input information used for the fit was exclusively based on very high-level ab initio calculations, CCSD(T)/cc-pVTZ.

First, for the two paths, abstraction and inversion, the new surface, named PES-2009, was subjected to stringent tests against the ab initio information: geometries, vibrational frequencies and energies of the stationary points, topology of the reaction paths, and the reaction swaths. In general, these ab initio data used for the fit are well reproduced by the new PES, showing the validity of the fitting procedure. The main difference is the bending angle at the saddle point for the abstraction reaction, which is not collinear in the ab initio level, while the surface predicts a collinear structure. However, we have shown that this limitation has no influence on the final kinetics results.

Second, as a first application of the use of the new PES, for both paths, abstraction and inversion, a kinetics study employing variational transition-state theory (TST) with multidimensional tunneling was performed over the temperature range 200−2000 K. For the hydrogen abstraction reaction, $NH_3 + H \rightarrow NH_2 + H_2$, the forward thermal rate constants showed excellent agreement with experiment, while the reverse rate constants appeared slightly underestimated. In the TST approach the reverse rate constant is obtained from the forward one by detailed balance, based on the equilibrium constant, K_{eq}. Given that the value of K_{eq} depends only on reactant and product properties with the reaction path properties canceling out, it is possible that quantum dynamics calculations for the reverse reaction would show better agreement with experiment. Finally, the kinetic isotope effects, $NH_3 + H/ND_3 + D$, reproduce the scarce experimental information available, which represent another severe test of the new PES.

Third, for the ammonia inversion reaction, the drawback of the old PES-1997 surface was avoided with the planar NH_3 (D_{3h}) structure energy now being above that of the pyramidal NH_3 (C_{3v}) structure. Because of tunneling, each degenerate vibrational level presents a splitting, ΔE. Our semiclassical calculations overestimate the experimental measurements, although they correctly predict the isotopic behavior, $NH_3 > ND_3$.

Finally, an exhaustive dynamics study using quasi-classical trajectory and quantum scattering dynamics calculations is currently under way, and its results will be reported in the near future. This dynamics study will be another severe test of the quality of the new PES developed in this paper.

In sum, the agreement (always qualitative and sometimes quantitative) obtained using the newly constructed surface with a wide spectrum of experimental measurements for both the reactions of hydrogen abstraction and ammonia inversion lends support to the polyatomic PES-2009 surface. The origin of the discrepancies was analyzed, concluding that some of them are due to flaws of the surface, but that some others could be attributed to limitations of the TST approach and/or to experimental uncertainties.

Acknowledgment. This work was partially supported by the Junta de Extremadura, Spain (Project No. PRI07A009).

References and Notes

(1) Dove, J. E.; Nip, W. S. *J. Chem. Phys.* **1974**, *52*, 1171.
(2) Michael, J. V.; Sutherland, J. W.; Klemm, R. B. *J. Phys. Condens. Matter* **1985**, *17*, 315.
(3) Marshall, P.; Fontijn, A. *J. Chem. Phys.* **1986**, *85*, 2637.
(4) Sutherland, J. W.; Michael, J. V. *J. Chem. Phys.* **1988**, *88*, 830.
(5) Ko, T.; Marshall, P.; Fontijn, A. *J. Phys.Chem.* **1990**, *94*, 1401.
(6) Friedrichs, G.; Wagner, H. G. *Z. Phys. Chem.* **2000**, *214*, 1151.
(7) Gordon, M. S.; Gano, D. R.; Boatz, J. A. *J. Am.Chem.Soc.* **1983**, *105*, 5771.
(8) Leroy, G.; Sana, M.; Tinant, A. *Can. J. Chem.* **1985**, *63*, 1447.
(9) Garrett, B. C.; Koszykowsky, M. L.; Melius, C. F.; Page, M. *J. Phys.Chem.* **1990**, *94*, 7096.
(10) Espinosa-Garcia, J.; Corchado, J.C. *J. Chem. Phys.* **1994**, *101*, 1333.
(11) Corchado, J. C.; Espinosa-Garcia, J. *J. Chem. Phys.* **1997**, *106*, 4013.
(12) Moyano, G. E.; Collins, M. A. *Theor. Chem. Acta* **2005**, *113*, 225.
(13) Li, H.; Liu, X.-G.; Zhang, Q.-G. *Chin. Phys. Lett.* **2005**, *22*, 1093.
(14) Zhang, X.-Q.; Cui, Q.; Zhang, J. Z. H.; Han, K.L. *J. Chem. Phys.* **2007**, *126*, 234304.
(15) Yang, M.; Corchado, J. C. *J. Chem. Phys.* **2007**, *126*, 214312.
(16) Yang, M.; Corchado, J. C. *J. Chem. Phys.* **2007**, *127*, 184308.
(17) Yang, M. *J. Chem. Phys.* **2008**, *129*, 064315.

(18) Willis, C.; Boyd, A. W.; Miller, O. A. *Can. J. Chem.* **1969**, *47*, 3007.
(19) Kurilo, M. J.; Holliden, G. A.; Lefevre, H. F.; Timmons, R. B. *J. Chem. Phys.* **1969**, *51*, 4497.
(20) Townes, C. H.; Schawlow, A. L. *Microwave Spectroscopy*; McGraw-Hill: New York, 1955.
(21) Dennisson, D. M.; Uhlenbeck, G. E. *Phys. Rev.* **1932**, *41*, 313.
(22) Rauk, A.; Allen, L. L.; Mislow, K. *Angew. Chem. Int. Ed.* **1970**, *9*, 400.
(23) Bunker, P. R.; Kraemer, W. P.; Spirko, V. *Can. J. Phys.* **1984**, *62*, 1801.
(24) Brown, F. B.; Tucker, S. C.; Truhlar, D. G. *J. Chem. Phys.* **1985**, *83*, 4451.
(25) Campoy, G.; Palma, A.; Sandoval, L. *Int. J. Quantum Chem. Quantum Chem. Symp.* **1989**, *23*, 355.
(26) Wormer, P. E. S.; Olthof, E. H. T.; Engeln, R. A. H.; Ress, J. *J. Chem. Phys.* **1993**, *178*, 189.
(27) Rush, D. J.; Wiberg, K. B. *J. Phys. Chem.* **1997**, *101*, 3143.
(28) Ghosh, D. C.; Jana, J.; Biswas, R. *Int. J. Quantum Chem.* **2000**, *80*, 1.
(29) Halpern, A. M.; Glendening, E. D. *Chem. Phys. Lett.* **2001**, *333*, 391.
(30) Halpern, A. M.; Ramachandran, B. R.; Glendening, E. D. *J. Chem. Educ.* **2007**, *84*, 1067.
(31) Swalen, J. D.; Ibers, J. A. *J. Chem. Phys.* **1962**, *36*, 1914.
(32) Morino, Y.; Kuchitsu, K.; Yamamoto, S. *Spectrochim. Acta Part A* **1968**, *24*, 335.
(33) Damburg, R. J.; Propin, R. K. *Chem. Phys. Lett.* **1972**, *14*, 82.
(34) Bopp, P.; McLaughlin, D. R.; Wolfsberg, M. *Z. Naturforsch Teil A* **1982**, *37*, 398.
(35) Spirko, V. *J. Mol. Spectrosc.* **1983**, *101*, 30.
(36) Maessen, B.; Bopp, P.; McLaughlin, D. R.; Wolfsberg, M. *Z. Naturforsch. Teil A* **1984**, *39*, 1005.
(37) Leonard, C.; Carter, S.; Handy, N. C. *Chem. Phys. Lett.* **2003**, *370*, 360.
(38) Kendall, R. A.; Dunning, T. H.; Harrison, R. J. *J. Chem. Phys.* **1992**, *96*, 6796.
(39) Schatz, G. C.; Amaee, B.; Connor, J. N. L. *J. Chem. Phys.* **1990**, *92*, 4893.
(40) Troya, D.; Pascual, R. Z.; Schatz, G. C. *J. Phys. Chem. A* **2003**, *107*, 10497.
(41) Corchado, J. C.; Chuang, Y.-Y.; Coitiño, E. L.; Ellingson, B. A.; Truhlar, D. G. *Gaussrate 9.5*; University of Minnesota: Minneapolis, 2007.
(42) Frisch, M. J.; Trucks, G. W.; Schlegel, H. B.; Scuseria, E.; Robb, M. A.; Cheeseman, J. R.; Zakrzewski, V. G.; Montgomery, J. A.; Stratman, R. E.; Burant, J. C.; Dapprich, S.; Millam, J. M.; Daniels, A. D.; Kudin, K. N.; Strain, M. C.; Farkas, O.; Tomasi, J.; Barone, V.; Cossi, M.; Cammi, R.; Menucci, B.; Pomelli, C.; Adamo, C.; Clifford, S.; Ochterki, J.; Petterson, G. A.; Ayala, P. Y.; Cui, Q.; Morokuma, K.; Malik, D. K.; Rabuk, A. D.; Raghavachari, K.; Foresman, J. B.; Cioslowski, J.; Ortiz, J. V.; Stefanov, J. J.; Liu, G.; Liashenko, A.; Piskorz, P.; Komaromi, I.; Gomperts, R.; Martin, R. L.; Fox, D. J.; Keith, T.; Al-Laham, M. A.; Peng, C. Y.; Nanayakkara, A.; González, C.; Challacombe, M.; Gill, P. M. W.; Johnson, B. G.; Chen, W.; Wong, M. W.; Andres, J. L.; Head-Gordon, M.; Reploge, E. S.; Pople, J. A.; *GAUSSIAN 03 Program*, Revision B.5; Gaussian Inc.: Pittsburgh, PA, 2003.
(43) Corchado, J. C.; Chuang, Y.-Y.; Fast, P. L.; Hu, W.-P.; Liu, Y.-P.; Lynch, G. C.; Nguyen, K. A.; Jackels, C. F.; Fernandez-Ramos, A.; Ellingson, B. A.; Lynch, B. J.; Melissas, V. S.; Villà, J.; Rossi, I.; Coitiño, E. L.; Pu, J.; Albu, T.; Steckler, R.; Garrett, B. C.; Isaacson, A. D.; Truhlar, D. G. *Polyrate 9.5*; University of Minnesota: Minneapolis, 2007.
(44) Kraka, E.; Gauss, J.; Cremer, D. *J. Chem. Phys.* **1993**, *99*, 5306.
(45) Truhlar, D. G. *Chem. Phys. Lett.* **1998**, *294*, 45.
(46) Fast, P. L.; Sanchez, M. L.; Truhlar, D. G. *J. Chem. Phys.* **1999**, *111*, 2921.
(47) Corchado, J. C.; Bravo, J. L.; Espinosa-Garcia, J. *J. Chem. Phys.* **2009**, *130*, 184314.
(48) Espinosa-Garcia, J. *J. Phys. Chem. A* **2001**, *105*, 134.
(49) Espinosa-Garcia, J. *J. Phys. Chem. A* **2001**, *105*, 8748.
(50) Page, M.; McIver, J. W. *J. Chem. Phys.* **1988**, *88*, 922.
(51) Fast, P. L.; Truhlar, D. G. *J. Chem. Phys.* **1998**, *109*, 3721.
(52) Jackels, C. F.; Gu, Z.; Truhlar, D. G. *J. Chem. Phys.* **1995**, *102*, 3188.
(53) Chuang, Y.-Y.; Truhlar, D. G. *J. Phys. Chem. A* **1998**, *102*, 242.
(54) Garrett, B. C.; Truhlar, D. G. *J. Am. Chem. Soc.* **1979**, *101*, 4534.
(55) Truhlar, D. G.; Isaacson, A. D.; Garrett, B. C. In *Theory of Chemical Reaction Dynamics*; Baer, M., Ed.; Chemical Rubber Co.: Boca Raton, FL, 1985; Vol. 4, p 65.
(56) Liu, Y.-P.; Lynch, G. C.; Truong, T. N.; Lu, D.-h.; Truhlar, D. G. *J. Am. Chem. Soc.* **1993**, *115*, 2408.
(57) Fernandez-Ramos, A.; Truhlar, D. G. *J. Chem. Phys.* **2001**, *114*, 1491.
(58) Demissy, M.; Lesclaux, R. *J. Am. Chem. Soc.* **1980**, *102*, 2897.
(59) Hack, W.; Rouverirolles, P.; Wagner, H. G. *J. Phys. Chem.* **1986**, *90*, 2505.
(60) *JANAF Thermochemical Tables*, 3rd ed.; Chase, M. W., Jr., Davies, C. A., Downey, J. R., Frurip, D. J., McDonald, R. A., Syverud, A. N., Eds.; National Bureau of Standards: Washington, DC, 1985; Vol. 14.
(61) Espinosa-Garcia, J.; Corchado, J. C.; Marquez, A. *Chem. Phys. Lett.* **1995**, *233*, 220.
(62) Defrees, D. J.; Hehre, W. J.; McIver, R. T.; McDanile, D. H. *J. Phys. Chem.* **1979**, *83*, 232.
(63) Carson, A. S.; Laye, P. G.; Yurekli, M. *J. Chem. Thermodyn.* **1977**, *9*, 827.
(64) Dixon, D. A.; Feller, D.; Peterson, K. A. *J. Chem. Phys.* **2001**, *115*, 2576.
(65) Song, Y.; Qian, X.-M.; Lan, K. C.; Ng, Y. C.; Liu, J.; Chen, W. *J. Chem. Phys.* **2001**, *115*, 2582.
(66) Marshall, P.; Fontijn, A. *J. Phys. Chem.* **1987**, *91*, 6297.
(67) Herzberg, G. *Molecular Spectra and Molecular Structure II*; Van Nostrand: Princeton, NJ, 1945; p 223.
(68) Gordy, W.; Cook, R. L. *Microwave Spectra*; Interscience: New York, 1970.
(69) Cleeton, C. E.; Williams, N. H. *Phys. Rev.* **1934**, *45*, 234.
(70) Pesonen, J.; Miani, A.; Halonen, L. *J. Chem. Phys.* **2001**, *115*, 1243.
(71) Kamarchik, E.; Wang, Y.; Bowman, J. *J. Phys.Chem. A* **2009**, *113*, 7556.
(72) Ragni, M.; Lombardi, A.; Pereira Barreto, P. R.; Peixoto Bitencourt, A. C. *J. Phys. Chem. A* **2009**, *113*, 15355.
(73) Davi, V. M.; Das, P. P.; Rao, K. N.; Urban, S.; Papouseck, D.; Spirko, V. *J. Mol. Spectrosc.* **1981**, *88*, 293.

JP1001513